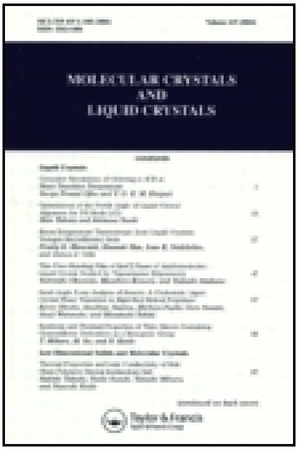

Molecular Crystals and Liquid Crystals
Publication details, including instructions for authors and subscription information:
http://www.tandfonline.com/loi/gmcl20

# Rheological Behavior of Azobenzene Nematic Homopolymer and Copolymer

Laura Andreozzi [a], Massimo Faetti [a], Marco Giordano [a], Fabio Zulli [a], Giancarlo Galli [b] & Michele Laus [c]

[a] Dipartimento di Fisica "E. Fermi" and INFM, Università di Pisa, Pisa, Italy

[b] Dipartimento di Chimica e Chimica Industriale, Università di Pisa, Pisa, Italy

[c] Dipartimento di Scienze e Tecnologie Avanzate, Università del Piemonte Orientale, Alessandria, Italy

Version of record first published: 31 Aug 2006

To cite this article: Laura Andreozzi, Massimo Faetti, Marco Giordano, Fabio Zulli, Giancarlo Galli & Michele Laus (2005): Rheological Behavior of Azobenzene Nematic Homopolymer and Copolymer, Molecular Crystals and Liquid Crystals, 429:1, 301-312

To link to this article: http://dx.doi.org/10.1080/15421400590931033

*Mol. Cryst. Liq. Cryst.*, Vol. 429, pp. 301–312, 2005
Copyright © Taylor & Francis Inc.
ISSN: 1542-1406 print/1563-5287 online
DOI: 10.1080/15421400590931033

# Rheological Behavior of Azobenzene Nematic Homopolymer and Copolymer

**Laura Andreozzi**
**Massimo Faetti**
**Marco Giordano**
**Fabio Zulli**
Dipartimento di Fisica "E. Fermi" and INFM, Università di Pisa,
Pisa, Italy

**Giancarlo Galli**
Dipartimento di Chimica e Chimica Industriale, Università di Pisa,
Pisa, Italy

**Michele Laus**
Dipartimento di Scienze e Tecnologie Avanzate, Università del Piemonte
Orientale, Alessandria, Italy

*A rheological study of a methacrylate homopolymer containing azobenzene side groups and its 70/30 copolymer with methyl methacrylate was performed in the linear viscoelastic regime. The creep and oscillatory measurements enabled us to obtain the temperature dependence of the zero shear viscosity* $\eta$. *The time-temperature superposition principle (TTS) was found to hold over large temperature intervals; in particular no discontinuities were detected at the isotropic-nematic transition in either sample. However, the homopolymer evidenced a peculiar signature in the shear elastic complex modulus* $G^*(\omega,T)$ *at a temperature* $T_c$ *in the nematic phase. This was attributed to a conformational transition driven by the nematic order.*

**Keywords:** azobenzene; conformational transition; liquid crystal polymer; nematic; rheology

Address correspondence to Laura Andreozzi, E-mail: laura.andreozzi@df.unipi.it

# INTRODUCTION

In the last years, side group liquid crystalline polymers have been deeply investigated because of their potential application as media for optical information storage [1,2]. In particular, liquid crystalline polymers with azobenzene side groups appeared to be suitable candidates to this aim [1,3]. We accomplished in fact optical writing at both micrometer and nanometer length scales in the nematic polymethacrylate PMA4 system, homopolymer and copolymers, that consists of an azobenzene side group [4–7] (Fig. 1).

Bit stability, homogeneity at molecular level, and working temperature range are crucial materials parameters to achieve an effective, high-resolution and long-term data storage [4,5]. Therefore, techniques that cover different time and length scales must be employed in order to fully characterize the polymer matrices of interest. For example, we investigated by ESR spectroscopy the dynamics of the cholestane spin probe in PMA4 homopolymer and copolymer and evidenced different signatures in the dynamics of the molecular tracer [4]. These were in turn correlated with the structural relaxation of the polymers as revealed by rheological measurements as function of temperature [5].

In the present work, we extended our rheological investigations of the dynamic shear and creep behaviors to cover the whole temperature range from the isotropic melt, across the nematic phase, down to the glassy state of PMA4 homopolymer and 70/30 copolymer and found that TTS principle holds through the whole investigated temperature range, even across the nematic-isotropic transition in either sample. However, the homopolymer exhibits a clear discontinuity at the conformational transition temperature $T_c$.

# MATERIALS AND EXPERIMENTAL

Both the PMA4 homopolymer and the 70/30 copolymer ($x = 0.7$) samples were prepared by free-radical polymerization according to a

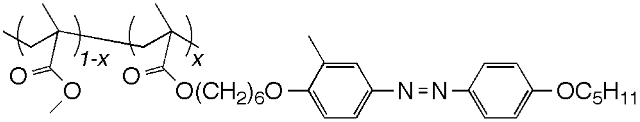

**FIGURE 1** Structure of the PMA4 homopolymer ($x = 1$) and 70/30 copolymer ($x = 0.7$).

**TABLE 1** Physico-chemical Characteristics of the PMA4 Polymer Samples

| PMA4 Sample | $M_w$(g/mol) | $M_w/M_n$ | $T_g$(K) | $T_c$(K) | $T_{NI}$(K) |
|---|---|---|---|---|---|
| Homopolymer | 59000 | 3.17 | 294 | 320 | 353 |
| 70/30 Copolymer | 117000 | 3.54 | 314 | — | 345 |

literature procedure [8]. Their physico-chemical characteristics are reported in Table 1.

The average molar masses were determined by size exclusion chromatography with polystyrene standards. Differential scanning calorimetry (DSC) measurements were performed with a Perkin-Elmer DSC7 calorimeter (10 K/min heating rate) frequently calibrated with indium and zinc standards. For the homopolymer, in addition to the glass transition temperature $T_g$ and the nematic-isotropic temperature $T_{NI}$, the DSC traces also evidenced a change in heat capacity associated to a backbone conformational transition at the onset temperature $T_c$ of 320 K [5] (Fig. 2). Previous LODESR spectroscopy studies suggested that this transition was driven by the increasing

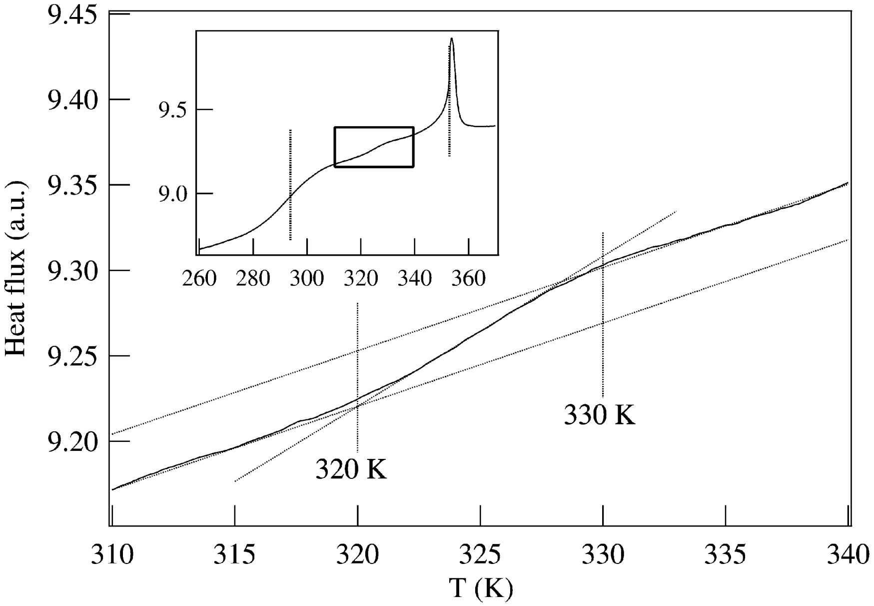

**FIGURE 2** DSC heating scan for PMA4 homopolymer with the enlarged 310–340 K region (10 K/min rate).

nematic order as the temperature was lowered [7]. This transition is not observed in the copolymer where the strength of the nematic potential is reduced by the presence of non-mesogenic groups.

Rheological measurements, both continuous and oscillatory, were carried out with a Haake RheoStress RS150H rheometer in the plane-plate geometry (20 mm diameter) in the temperature range 303–403 K under highly pure nitrogen flow. In order to account for thermal dilatation of the system, the gap in the plane parallel geometry was automatically varied in the temperature range between 0.40 μm and 0.60 μm. The gap was chosen significantly larger than the chain length to ensure gap independent measurements. The sample temperature was stable within 0.1 K.

Preliminary tests on viscoelastic linearity of the materials were conducted, which guaranteed that all measurements were carried out in the linear regime. Zero shear viscosity was obtained in two independent ways by i) creep measurements at different temperatures, and ii) loss modulus $G''$ resulting from frequency sweep measurements. The temperature dependences of the structural relaxation time $\tau^{st}$ in the investigated regions were well described by the Vogel-Fulcher (VF) law:

$$\tau^{st} = \tau_0^{st} \exp\left(\frac{T_b}{T - T_0}\right) \tag{1}$$

$T_0$ and $T_b$ being the Vogel temperature and the activation pseudo-energy (in K), respectively. The relevant parameters in Eq. (1) $T_0 = 259 \pm 5\,\mathrm{K}$, $T_b = 1300 \pm 50\,\mathrm{K}$ and $\tau_0^{st} = (7.0 \pm 0.8) \cdot 10^{-13}\,\mathrm{s}$ for the homopolymer, and $T_0 = 266 \pm 5\,\mathrm{K}$, $T_b = 1570 \pm 50\,\mathrm{K}$ and $\tau_0^{st} = (1.7 \pm 0.2) \cdot 10^{-12}\,\mathrm{s}$ for the copolymer.

## THEORETICAL BACKGROUND

According to the TTS principle [9], the dependence of the shear elastic complex modulus on $\omega$ and $T$ can be written as:

$$G^*(\omega, T) = b_{Tr}(T) G^*(a_{Tr}(T)\omega, T_r) \tag{2}$$

as a function of shear elastic complex modulus measured at the reference temperature $T_r$. The vertical and horizontal shift parameters, $b_{Tr}(T)$ and $a_{Tr}(T)$, are two real temperature dependent functions. While $a_{Tr}(T)$ is a frequency shift factor that strongly depends on temperature, the $b_{Tr}(T)$ factor is usually a very weak function of temperature and its value is very close to $T/T_r$; thus $b_{Tr}(T)$ is commonly replaced by one and neglected in not too wide temperature ranges.

Horizontal and vertical shift factors at the reference temperature, as well as master curves, are obtained by a mathematical shift of the experimental isothermal frequency sweeps of $G^*(\omega)$ [10].

The relaxation of a real viscoelastic material is ruled by the law for the complex modulus $G^*(\omega)$ in the frequency regime at the reference temperature [11]:

$$G^* = G_\infty \int_{-\infty}^{+\infty} \frac{\omega^2\tau^2 + i\omega\tau}{1+\omega^2\tau^2}\rho(\tau)d(\ln\tau) \tag{3}$$

where $\rho$, $\omega$, $\tau$, and $G_\infty$ are real valued. By defining:

$$\langle\tau\rangle = \int_{-\infty}^{+\infty} \tau\rho(\tau)d(\ln\tau) \tag{4}$$

and remembering that the zero shear viscosity $\eta$ is given by the limit:

$$\eta = \lim_{\omega\to 0}\frac{G''(\omega)}{\omega} \tag{5}$$

from Eqs. (3) and (4) one finds:

$$\eta(T_r) = G_\infty(T_r)\langle\tau(T_r)\rangle \tag{6}$$

Therefore, being $\eta(T) = a_{Tr}(T)\ b_{Tr}(T)\ \eta(Tr)$ [9], it also holds:

$$\eta(T) = a_{Tr}(T)\ b_{Tr}(T)\ G_\infty(T_r)\langle\tau(T_r)\rangle \tag{7}$$

which leads to determine the value of the viscosity in the whole temperature range. The relaxation time distribution $\rho(\tau,T_r)$ is calculated from master curves with a nonlinear regularization method [11,12]. Through this distribution, $\langle\tau(T_r)\rangle$ is derived as well.

## RESULTS AND DISCUSSION

The rheological measurements were performed in the temperature ranges of 303–403 K and 323–394 K for the homopolymer and the 70/30 copolymer, respectively, with reference temperatures at the same $T_r/T_g$ ratio ($T_r = 363$ K for the homopolymer and $T_r = 388$ K for the copolymer). As shown in Figure 3 (and later on in Fig. 6), single master curves were found for the storage $G'$ and loss $G''$ moduli in both the nematic and isotropic phases for the two polymer samples.

This finding indicates that the rheological properties are dominated by the polymer backbone [13]. In both homopolymer and copolymer master curves a liquid behavior is observed in the low frequency side, with no evidence in the overall frequency range of any rubbery plateau characteristic of entanglement effects. Entanglement could have been

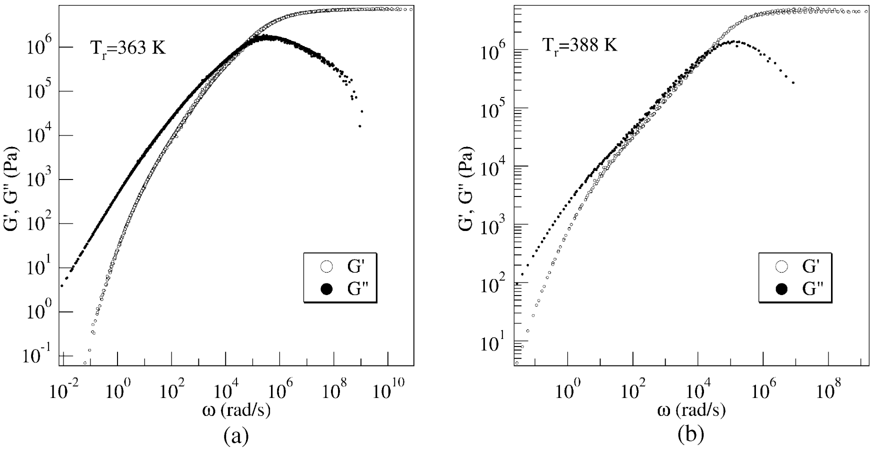

(a) (b)

**FIGURE 3** Master curves of storage (empty circles) and loss moduli (filled circles) for the PMA4 homopolymer at $T_r = 363\,\mathrm{K}$ (a) and copolymer at $T_r = 388\,\mathrm{K}$ (b).

expected especially in the copolymer as in various acrylic polymers such a plateau first appears roughly at the critical molar mass $M'_{\mathrm{c}} \sim 3 \bullet M_{\mathrm{e}} \sim 26000\,\mathrm{g/mol}$ [14], with $M_e$ the entanglement mass. It is worth noting that absence of entanglement was also inferred from the master curves of several analogous azobenzene polymethacrylates [15], even at molecular weights expected to be above $M'_{\mathrm{c}}$. We suggest that the nematic order dilates the confining tube, on which dimension the $M_{\mathrm{e}}$ value depends [14], and shifts entanglement to higher molar masses.

However for the 70/30 copolymer, the loss and storage modulus master curves were quite parallel over a wide frequency range, following the power law $G'$, $G'' \sim \omega^{1/2}$. This behavior confirms the modified Rouse theory for undiluted polymers and is a known property for polymers with molecular weights near the minimum values for entanglement coupling in the region between the terminal zone and the glassy zone [9].

Figure 4 shows the distributions of the relaxation times $\rho(\tau)$ for the homopolymer and the copolymer at the reference temperature; the structural, the terminal and the average times are also marked. The structural times follow the VF law of Eq. (1) with the pertinent parameters given above. Moreover, we found $\langle\tau\rangle$ 60 µs and 0.6 ms, $G_\infty$ $7.2 \cdot 10^6$ Pa and $4.5 \cdot 10^6$ Pa, and $\eta$ 450 Pa · s and 2800 Pa · s for the homopolymer and the copolymer, respectively, which also provide confirmation to Eq. (6).

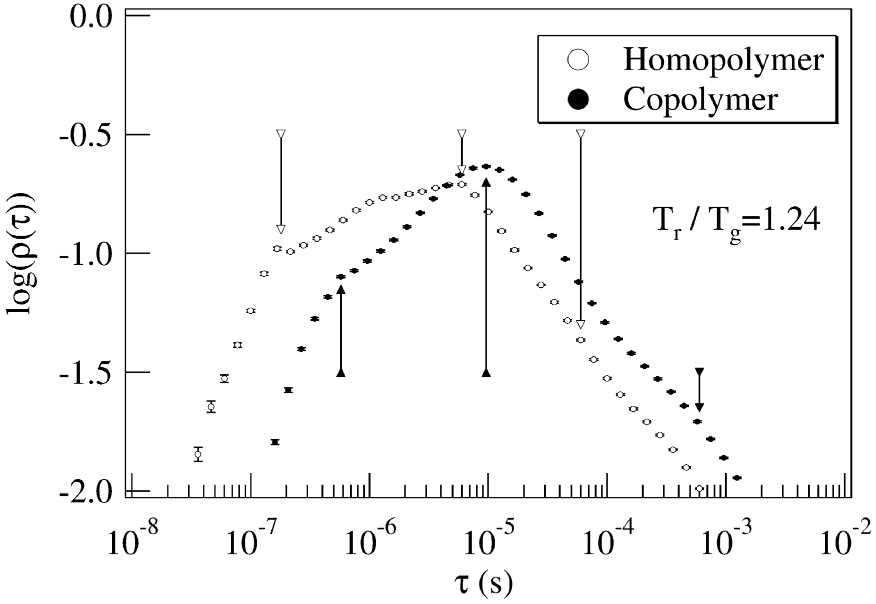

**FIGURE 4** Relaxation time distributions $\rho(\tau)$ of PMA4 homopolymer (empty circles) and copolymer (filled circles). The arrows mark the respective structural, terminal and average times (from shorter to longer times).

The values of viscosity obtained by oscillatory measurements and direct creep measurements are plotted vs. $1/T$ in Figure 5. No discontinuity of the viscosity was observed at the $T_{NI}$ in either sample. As the $T_g$ was approached, creep measurements of different lengths of time were performed and their comparisons are also reported in Figure 5. It is well known that, on lowering the temperature, creep measurements require longer times to attain the steady shear flow regime, where $G''$ is proportional to $\omega$. In our experiments the longer the creep time was, the better the agreement was of the measured viscosity with the oscillatory data (Fig. 5). In particular, times of the order of magnitude of $10^5$ s were taken for reliable creeps of the copolymer at the two lowest temperatures investigated, 328 K and 323 K. An analogous behavior was exhibited by the homopolymer at the temperature of 303 K. The longest creep, lasting 1 day, showed that the shear viscosity value very well agreed with the one obtained by the oscillatory measurements.

This agreement and the fact that the master curves in the different phases were well superimposable (Fig. 6) confirm that the TTS

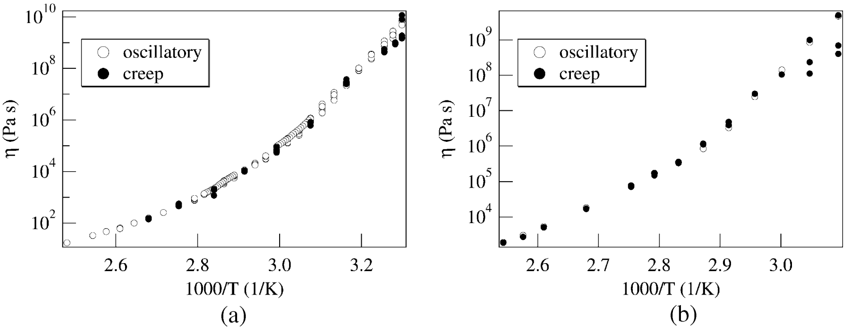

**FIGURE 5** Zero shear viscosity for the hompolymer (a) and copolymer (b). The oscillatory points are open symbols and the creep points are bullets.

principle also holds for these side group polymers, in agreement with previous results on similar liquid crystal polymers [13,15]. In fact, it was found that the TTS failed at the nematic-isotropic transition in polymers possessing very high molar masses [13]. The present

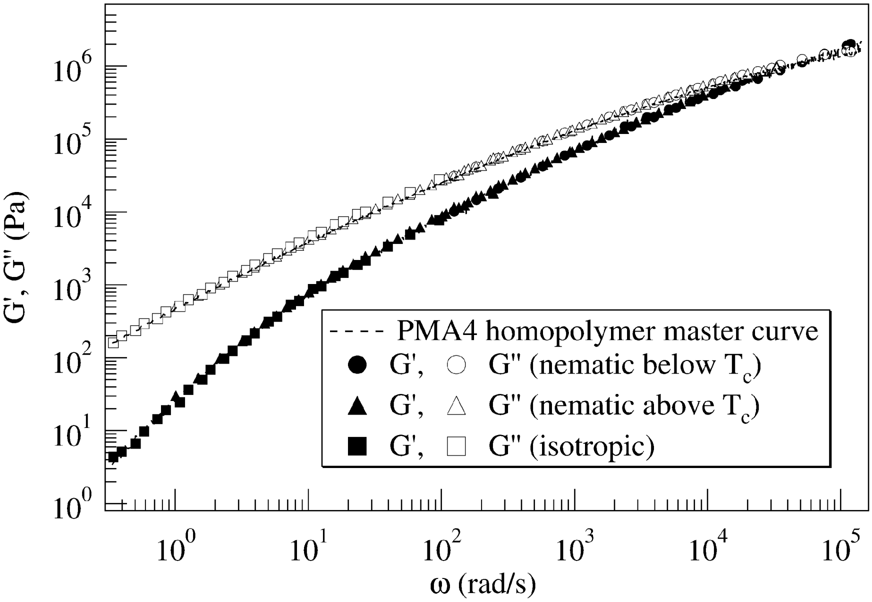

**FIGURE 6** Superimposed master curves for the homopolymer at various reference temperatures in different phases: isotropic (squares), nematic above $T_c$ (triangles), nematic below $T_c$ (circles).

PMA4 samples both have molecular weights at least one order of magnitude lower than those of the samples for which TTS fails [13].

After having verified the validity of the TTS principle even across the phase transition temperature (Fig. 6), we noted a peculiar phenomenon in the vertical shift parameter $b_{Tr}(T)$ for the homopolymer. Usually the $b_{Tr}(T)$ plots are very unstructured with varying temperature and consist of slightly scattered points around the reference line $T/T_r$. It is well known that this vertical correction factor accounts for the changes with temperature of the unrelaxed and/or relaxed shear modulus [16], which usually depend only on the small density variations with temperature. However, this behavior is not followed by PMA4 homopolymer, for which the $b_{363K}(T)$ mean value doubles within a narrow range of 6 K when crossing the temperature of 328 K (Fig. 7).

It is important to note that previous ESR and LODESR studies of the homopolymer dynamics had suggested [4,7] that, on lowering temperature, a conformational transition of the polymer backbone took place in this same range of temperature, driven by the increasing nematic order in the side groups. This finding is also consistent with the DSC thermogram shown in Figure 2, where a conformational change in the main chain polymer appeared to occur in the 320–330 K temperature range. This additional phenomenon appears to

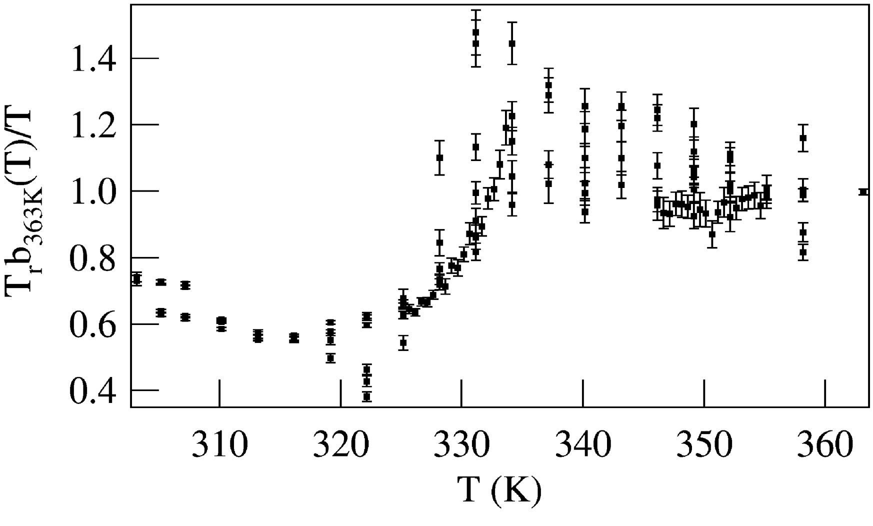

**FIGURE 7** Temperature dependence of the vertical shift parameter $b_{363K}(T)$ for the PMA4 homopolymer.

alter the usual trend of $b_{Tr}(T)$ observed in amorphous linear polymers, revealing itself as a not- trivial temperature dependence of the limiting modulus. As a consequence of the conformational transition, an increase in the polymer main chain rigidity is expected at lower temperatures below $T_c$.

Evidence that the polymer is more rigid below $T_c$ is provided by the data in Figure 8, which illustrates an oscillatory temperature scan. The trend of $G'$ with temperature, at the fixed frequency of 10 Hz, clearly shows a plateau at $\approx 10^7$ Pa up to $T_g$ and a second plateau at $\approx 6 \cdot 10^6$ Pa down to approximately $T_c$. Interestingly enough, the $G'$ value in the plateau regions approximately doubles, the same factor having been observed in the trend of $b_{Tr}(T)$. A pronounced drop in modulus is then detected as the temperature is increased in the nematic phase. The 10 Hz measurements are on a time scale fast with respect to the polymer dynamics around the $T_g$, and the glassy plateau lasts for several degrees above the glass transition temperature determined by DSC measurements. However, in the vicinity of the

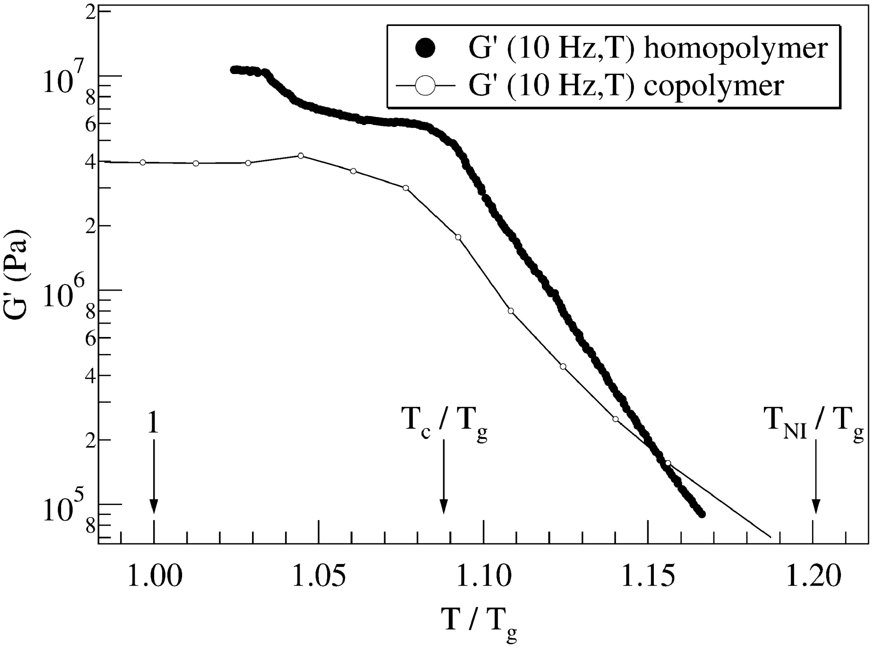

**FIGURE 8** Temperature scan of storage modulus at the constant frequency of 10 Hz for the PMA4 homopolymer and copolymer. The marks refer to the transition temperatures for the homopolymer.

$T_c$ the polymer dynamics is fast enough with respect to 10 Hz oscillatory measurements and the conformational crossover is signaled more precisely. One should note that such a peculiar behavior does not occur in the 70/30 copolymer in which the presence the non-mesogenic methyl methacrylate co-units as side groups would inhibit the conformational transition of the polymer main backbone.

## CONCLUSIONS

We have shown that the time-temperature superposition principle holds over the whole temperature range investigated, and in particular across the nematic-isotropic transition for both the homopolymer and the copolymer. However, the homopolymer evidence a transition at $T_c$ that can not be detected in the copolymer. Below such conformational transition the rigidity of the polymeric matrix, as measured by $G'$, increases to a level comparable to that at $T_g$. The reduced conformational freedom would allow, in turn, to better stabilize photoimprinted information at higher temperatures as observed in [17].

## REFERENCES

[1] Nakano, M., Yu, Y., Shishido, A., Tsutsumi, O., Kanazawa, A., Shiono, T., & Ikeda, T. (2003). *Mol. Cryst. Liq. Cryst.*, *398*, 1. (b) Residori, S. & Petrossian, A. (2003). *Mol. Cryst. Liq. Cryst.*, *398*, 137.

[2] Yamane, H., Kikuchi, H., & Kajiyama, T. (1999). *Polymer*, *40*, 4777.

[3] Bubliz, D., Helgert, M., Fleck, B., Wenke, L., Hvilsted, S., & Ramanujam, P. S. (2000). *Appl. Phys. B*, *70*, 803. (b) Wuestneck, R., Stumpe, J., Karageorgieva, V., Meier, L. G., Rutloh, M., & Presher, D. (2002). *Coll. Surf. Physicochem. Engineer. Asp.*, *198–200*, 753.

[4] Andreozzi, L., Faetti, M., Galli, G., Giordano, M., & Palazzuoli, D. (2004). *Macromol. Symp.* in press and references therein.

[5] Andreozzi, L., Faetti, M., Galli, G., Giordano, M., & Palazzuoli, D. (2001). *Macromolecules*, *34*, 7325.

[6] Likodimos, V., Labardi, M., Pardi, L., Allegrini, M., Giordano, M., Arena, A., & Patanè, S. (2003). *Appl. Phys. Lett.*, *82*, 3313.

[7] Andreozzi, L., Bagnoli, M., Faetti, M., & Giordano, M. (2001). *Mol. Cryst. Liq. Cryst.*, *372*, 1.

[8] Angeloni, A. S., Caretti, D., Laus, M., Chiellini, E., & Galli G. (1991). *J. Polym. Sci., Polym. Chem. Ed.*, *29*, 1865.

[9] Ferry, J. D. (1980). *Viscoelastic properties of polymers*, Wiley: New York.

[10] Honerkamp, J. & Weese, J. (1993). *Rheol. Acta*, *32*, 57.

[11] Honerkamp, J. & Weese, J. (1993). *Rheol. Acta*, *32*, 65.

[12] Weese, J. (1993). *J. Comput. Phys. Commun.*, *77*, 429.

[13] Berghausen, J., Fuchs, J., & Richtering, W. (1997). *Macromolecules*, *30*, 7574.

[14] Fetters L. J., Lohse D. J., Richter, D., Witten, T. A., & Zirkel A. (1994). *Macromolecules*, *27*, 4639.

[15] Colby, R. H., Gillmor, J. R., Galli, G., Laus, M., Ober, C. K., & Hall, E. (1993). *Liq. Cryst.*, *13*, 233.

[16] McCrum N. G., Read B. E., & Williams, G. (1991). *Anelastic and dielectric effects in polymeric solids*, Dover: New York, from 127.

[17] Andreozzi, L., Faetti, M., Giordano, M., Palazzuoli, D., Laus, M., & Galli. G. (2003). *Mol. Cryst. Liq. Cryst.*, *398*, 97.